Design Optimization and Evaluation of a 64-Channel Cardiac Array Coil at 3T

Robin Etzel[1,2], Xueming Cao[1,3], Choukri Mekkaoui[1], David E. Sosnovik[1], Timothy G. Reese[1], Mark Schuppert[4], Laura M. Schreiber[4,5], Martin Fiebich[2], Lawrence L. Wald[1], and Boris Keil[1]

[1]A.A. Martinos Center for Biomedical Imaging, Dept. of Radiology, Massachusetts General Hospital, Harvard Medical School, Charlestown, MA, United States, [2]Mittelhessen University of Applied Sciences, Institute for Medical Physics and Radiation Protection, Giessen, Germany, [3]Medical Physics, Department of Radiology, University Medical Center Freiburg, Freiburg, Germany, [4]Department of Radiology, Johannes Gutenberg University Medical Center, Section of Medical Physics, Mainz, Germany, [5]Comprehensive Heart Failure Center, Department of Cellular and Molecular Imaging, Wuerzburg, Germany

Audience: RF coil engineers, MRI Cardiologists, students and trainees in MRI coils

Introduction: In cardiac MRI, parallel acquisition has impacted clinical applications such that nearly every cardiac examination is performed with an array comprising multiple surface coil elements. In experimental settings, this has been followed up with high-density cardiac arrays with up to 128 channels [1]. Recent state-of-the-art MRI scanners utilize 64 channels and can therefore provide the ability to translate latest research in coil technology to clinical cardiac MRI studies. A number of technical issues arise in the implementation of large channel-count arrays employing relatively small element sizes. One major constraint of cardiac arrays is the loss of the ability to use fully flexible body coil former due to the high-density of implemented rigid components, e.g. preamplifiers or solder joints. However, totally rigid array coils potentially underperform on subjects, when they do not match the sizing of the coil former. In a previous study we explored a 64ch cardiac array on a rigid former design [2]. In this study, we designed a semi-adjustable anatomical-shaped 64ch cardiac array coil in order to maintain close-fitting receive elements across different body shapes. The constructed coil was developed in a way that addresses patient comfort concerns and can be disseminated for robust daily use.

Fig.1: 3D coil model and constructed 64-channel cardiac coil array

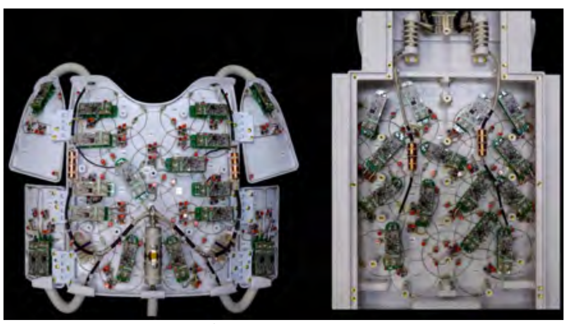

Fig.2: Close-up of anterior and posterior coil portion

Material and Methods: The constructed coil consists of two independent shell-like housing segments. The posterior portion houses 28 circular elements and follows smoothly the contour of the human back and shoulder area. The anterior section houses 36 elements and is further divided up into five segments, where a main body former is linked to four adjustable lateral wings (shoulder and thorax). The latter allows adaptability to different body shapes. For large subjects the shoulder wings are folded out, while the lower wings can be placed between thorax and arms. Small subjects take advantage of the coil's adapting ability to be closely wrapped up by all anterior coil segments (all coil wings folded in). The coils were arranged in a overlapped array of hexagonal symmetry to minimize next neighbor coupling. The regular coil element's diameter is 92 mm, few coil elements are irregular shaped, because of the inner contour of the housing. Each loop inductance was divided symmetrically with discrete components into three segments (2x tuning capacitors and the output circuit with matching capacitors and active/passive detuning trap). While nearest neighbor decoupling was addressed with critical overlap where possible, next-nearest neighboring coil elements were decoupled using preamplifier decoupling [3] by transforming the low impedance of the preamplifier to an open circuit in the loop using a 5.5cm long coax cable and a series capacitor. Pairs of coils were attached to a preamplifier pair sharing a circuit board, which also served to mix the detected signal to an intermediate frequency and frequency domain multiplex the two channels onto a single coaxial output. Initial testing was done on a 3T Siemens Skyra MRI system (Siemens AG, Healthcare Sector). For SNR and G-factor comparison, PD-weighted GRE protocol (TR/TE/α =200 ms/4.03ms/20°, FoV=400 mm, 10 mm slice thickness, Matrix size: 256 x 256) were obtained using a custom body phantom. Data were compared to a 34-ch commercially available upper body coil array. For DWI, the images were obtained using a fat-suppressed, zone-selected, diffusion-encoded stimulated echo (STE) sequence with 10 diffusion encoding directions, TE/TR=36 ms / 2R-R intervals, GRAPPA rate 2, b-value 500 s/mm2, resolution 3.1x3.1x10 mm3, and 10 averages, using multiple breath-holds. The images were obtained using spatiotemporal reconstruction.

Results: The coil shows nearest neighbors decoupling of -17dB and a preamplifier decoupling of -20dB. The Q_U/Q_L-ratio was measured to be 302/29=10.4. We measured a 1.15x SNR increase at the ROI of the heart, when compared to the 34ch commercially array (►Fig 3 *right*). ►Fig.3 *left* shows inverse G-factors of a 4-fold accelerated phantom image; roughly providing one additional unit of acceleration for a given noise amplification factor at target region. Initial cardiac DWI images (►4) show sufficient images quality and post-processing were possible

Conclusion: A 64-channel cardiac array coil was constructed, tested and compared to a 34-channel commercially available upper body coil array, The 64ch coil provides improvements in SNR and in highly accelerated imaging. Robust and compact design considerations were implemented to facilitate clinical studies. Thus, the highly parallel cardiac array is well-suited for cardiac studies with improved sensitivity.

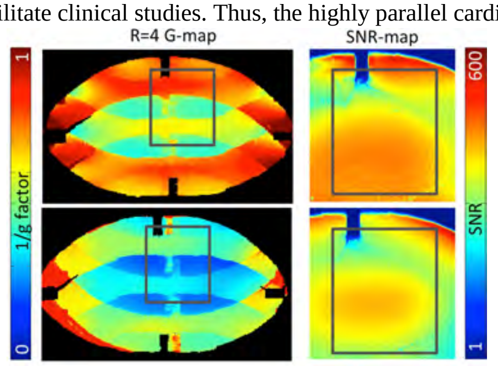

Fig.3: 1/G maps and SNR maps of phantom data

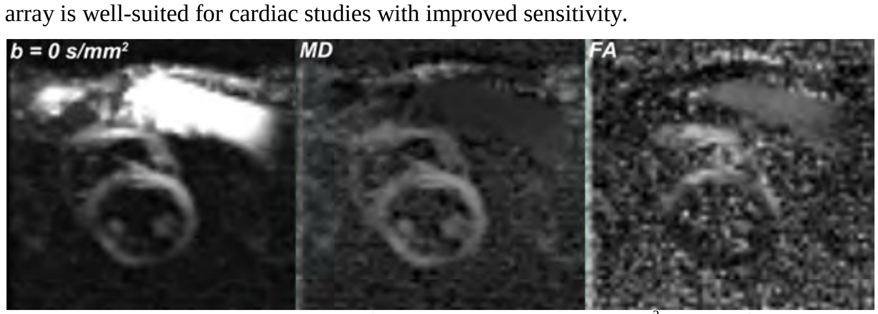

Fig.4: Midventricular short-axis view of a normal heart with a b=0 s/mm^2 image (left), MD map (middle), and FA map (right), demonstrating the ability to acquire cardiac diffusion tensor images with values of MD and FA that are within the established normal ranges.

References: [1] Schmitt M et al, MRM 59, 2008. [2] Schuppert et al ISMRM 2014 p 1315. [3] Roemer PB et al, MRM 16, 1990.